A two-dimensional time-dependent model for surface shear and buoyancy-driven flows in domains with large aspect ratio

Sumon K. Sinha* and Subrata Sengupta

Department of Mechanical Engineering, University of Miami, Coral Gables, FL 33124, USA
(Received March 1986; revised January 1987)

A two-dimensional numerical model has been developed for studying flows in enclosures having a large length-to-depth ratio. The model solves the two-dimensional Navier–Stokes and energy equations subject to hydrostatic, Boussinesq, and rigid-lid assumptions. Turbulent momentum and heat diffusion are incorporated using variable eddy coefficients. The flow is driven by surface wind shear and heat transfer. Two cases were run for a rectangular domain, subject to a suddenly imposed surface shear stress while the surface and bottom were maintained at two different but constant temperatures. The difference between the cases was the formulation used for predicting the eddy viscosities and diffusivities. The variations of velocities and temperatures with time were studied. Both velocities and temperatures were found to undergo a sudden rapid change, after an initial period of slow change, before attaining steady state. This has been explained in light of the differences in the convective and diffusive time scales and the nature of coupling between the governing equations.

Keywords: environmental flows

Introduction

Fluid flows in enclosures arising out of surface shear stress and heat transfer are usually found in all natural bodies of water (lakes, rivers, oceans, etc.). The length- (or width) to-depth ratio of such domains is usually high. The driving force in such flows arises out of meteorological impact on the surface combined with other inputs, such as concentration gradients and flow across domain boundaries.

Natural water bodies also exhibit density stratification due to changes in temperature and salinity. Various investigators have examined the interaction between stratification and fluid recirculation. Huppert and Linden[1] examined experimentally and numerically the stratification in a fluid with stable salinity gradient heated from below and developed a definition for effective conductivity of fluid layers. Brocard and Harleman[2] investigated experimentally and also developed a theoretical model for the convective circulation in a horizontal fluid layer closed at one end and driven by a constant buoyancy flux at the other end.

Horizontally integrated one-dimensional models have been used to investigate thermal stratification in lakes,

* Presently at Department of Mechanical Engineering, Florida International University, Miami, Florida 33199, USA.

0307-904X/87/050364-07/$03.00

among others, by Sundaram and Rehm,[3] Henderson-Sellers,[4] and Sengupta *et al.*[5] The mechanism for producing stratification in these studies is the vertical variation of eddy diffusivity, which in turn is related to the surface-wind-shear stress and vertical density gradients characterized by a Richardson number.

Experimental work on destratification in enclosures due to surface shear includes investigations of Sinha and Sengupta,[6] Koseff and Street,[7] Rhee *et al.*,[8] Kranenburg,[9,10] Kit *et al.*,[11] Wu,[12,13] Monismith,[14] and Chasechkin.[15] These studies incorporate recirculation due to the presence of end walls and have shown the flows to be three dimensional due to the presence of Taylor–Görtler-like instabilities in regions of high streamline curvature. Most laboratory studies, however, do not adequately model the large length-to-depth aspect ratio of natural water bodies. The studies of Koseff and Street[7] and Rhee *et al.*[8] were in square cavities. Increasing aspect ratios can drastically change the flow. This has been demonstrated experimentally for unstratified flows by Sinha.[16] Field observations from real lakes include the studies of Mortimer[17] and Wedderburn.[18,19]

Steady-state, two-dimensional numerical investigations for buoyancy- and surface-shear-driven flows in rectangular cutouts have been obtained, among others, by Torrance *et al.*[20] and Young *et al.*[21] They used turbulent closures but failed to show the nature of coupling between the eddy coefficients and the governing equations. A review of numerical techniques for modelling flows in natural water bodies has been presented by Simons.[22] The period of oscillation of internal seiches for a stratified basin has been investigated numerically, using a three-dimensional model, by Davies.[23]

Numerical modelling of wind-driven circulation in lakes includes, among others, investigations of Cheng *et al.*,[24] Davies,[25] Sengupta and Lick,[26] and Sengupta.[28] A major obstacle in modelling such flows is the proper choice of turbulent closures. Davies[25] used a three-dimensional model where the vertical eddy diffusivities and eddy viscosities could be specified arbitrarily, and discovered that the predicted velocities and temperatures strongly depend on the values of the eddy coefficients. Additionally, a study by James[29] has shown that shallow domains are especially susceptible to the eddy-viscosity/diffusivity formulation used.

The aim of this paper is to investigate the effects of turbulence closures on the transient phenomena in a shallow domain, due to a suddenly imposed surface shear stress, in the presence of a stable temperature gradient. For simplicity a rectangular domain and a two-dimensional model have been used. Results have been obtained with two different eddy–viscosity/diffusivity formulations.

Governing equations

The governing equations include the two-dimensional continuity, momentum, and energy equations subject to hydrostatic and Boussinesq assumptions. The equations are normalized with respect to a vertically stretched coordinate system given by α, γ instead of x, z, where $\gamma = \tilde{z}/\tilde{h}(\tilde{x})$ $\tilde{h}(\tilde{x})$ = the local depth ($= H$ for a constant depth basin) and $\alpha = \tilde{x}/L$.

The final nondimensional equations are

$$\frac{\partial}{\partial\alpha}(hu) + h\frac{\partial\Omega}{\partial\gamma} = 0 \qquad \text{(continuity)}$$

$$\frac{\partial}{\partial t}(hu) + \frac{\partial}{\partial\alpha}(huu) + h\frac{\partial}{\partial\gamma}(\Omega u) = -h\frac{\partial P_s}{\partial\alpha} - hBx + \frac{1}{\mathrm{Re}}\frac{\partial}{\partial\alpha}\left(h\frac{\partial u}{\partial\alpha}\right) + \left(\frac{1}{\epsilon^2\,\mathrm{Re}}\right)\frac{1}{h}\frac{\partial}{\partial\gamma}\left(A_v^*\frac{\partial u}{\partial\gamma}\right) \qquad \text{(momentum)}$$

where

$$Bx = E_u\frac{\partial h}{\partial\alpha}\int_0^\gamma \rho\,\mathrm{d}\gamma + E_u h\frac{\partial}{\partial\alpha}\int_0^\gamma \rho\,\mathrm{d}\gamma - E_u\gamma\left(\frac{\partial h}{\partial\alpha}\right)\rho$$

Also

$$\frac{\partial p}{\partial\gamma} = E_u(1+\rho) \qquad \text{(hydrostatic equation)}$$

$$\frac{\partial}{\partial t}(hT) + \frac{\partial}{\partial\alpha}(huT) + h\frac{\partial}{\partial\gamma}(\Omega T) = \frac{1}{\mathrm{Pe}}\frac{\partial}{\partial\alpha}\left(h\frac{\partial T}{\partial\alpha}\right) + \left(\frac{1}{\mathrm{Pe}\,\epsilon^2}\right)\frac{1}{h}\frac{\partial}{\partial\gamma}\left(B_v^*\frac{\partial T}{\partial\gamma}\right)$$

(energy equation)

$$\tilde{\rho} = 1.029431 - 0.000020\tilde{T} - 0.0000048\tilde{T}^2$$

(equation of state)

(where $\tilde{T}$ is in degrees Celsius)

The transformed vertical velocity Ω is related to the actual nondimensional vertical velocity as follows:

$$w = \gamma\left(u\frac{\partial h}{\partial x}\right) + h\Omega \qquad \text{where } \Omega = \frac{\partial\gamma}{\partial t}$$

and

$$u = \tilde{u}/U_{\mathrm{ref}} \quad w = \tilde{w}/\epsilon U_{\mathrm{ref}} \quad t = \tilde{t}/t_{\mathrm{ref}} \quad x = \tilde{x}/L$$

$$z = \tilde{z}/H \quad h = \tilde{h}/H \quad \epsilon = H/L \quad B_v^* = B_v/B_{\mathrm{ref}}$$

$$\rho = (\tilde{\rho} - \rho_{\mathrm{ref}})/\rho_{\mathrm{ref}} \quad p = \tilde{p}/(\rho_{\mathrm{ref}}U_{\mathrm{ref}}^2)$$

$$T = (\tilde{T} - T_{\mathrm{ref}})/T_{\mathrm{ref}} \quad A_h^* = A_h/A_{\mathrm{ref}} \quad A_v^* = A_v/A_{\mathrm{ref}}$$

$$B_h^* = B_h/B_{\mathrm{ref}} \quad t_{\mathrm{ref}} = L/U_{\mathrm{ref}} \quad \mathrm{Re} = U_{\mathrm{ref}}L/A_{\mathrm{ref}}$$

$$\mathrm{Pr} = A_{\mathrm{ref}}/B_{\mathrm{ref}} = 1 \quad \mathrm{Pe} = \mathrm{Re}\cdot\mathrm{Pr} \quad E_u = gh/U_{\mathrm{ref}}^2$$

Sengupta[28] derived the equations for a three-dimensional case. The equations are solved by a finite difference technique using a staggered grid system for computational stability. Initial values of velocities and temperatures are specified, and the solutions are marched forward in time. A Dufort–Frankel scheme is used to overcome the diffusive stability criterion. Although the equations incorporate vertical stretching to accommodate uneven bottom topographies, we used a rectangular domain. Hence, the derivatives of h with respect to α vanish. The domain and the boundary conditions are shown in *Figure 1*. The staggered grid system is shown in *Figure 2*.

Since the equations are solved in the primitive form and a rigid-lid surface condition is used, the surface

pressures are no longer atmospheric. The horizontal pressure gradient term in the momentum equation has to be evaluated at every time step. To prevent computational errors from accumulating in estimating this term, we obtain a second-order ordinary differential equation by differentiating the vertically integrated momentum equation with respect to α, as shown below:

$$\frac{\partial^2 P_s}{\partial \alpha^2} = \frac{1}{h}\left(-\frac{\partial}{\partial \alpha}(A_x - C_x + X_p)\right) - \frac{1}{h}\frac{dh}{d\alpha}\frac{dP_s}{d\alpha} - \frac{\partial \Omega}{\partial t}\bigg|_{\gamma=0}$$

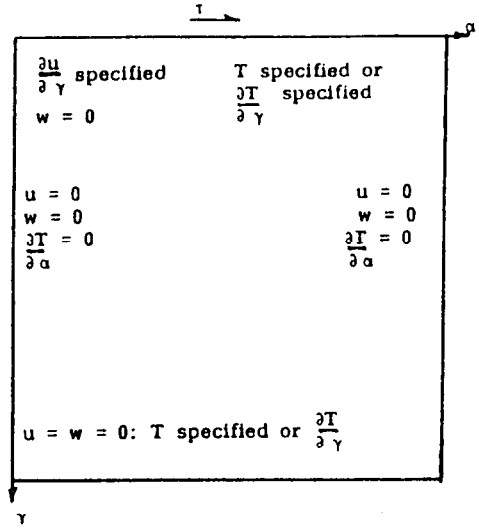

Figure 1 Boundary conditions

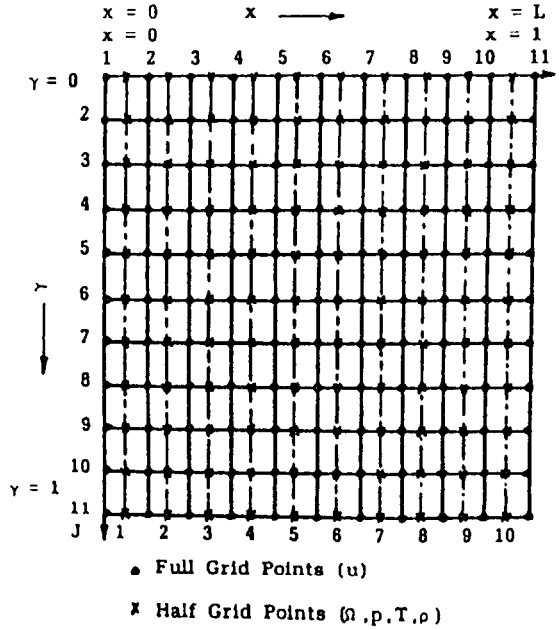

Figure 2 Finite difference grid system

where

$$A_x = \int_0^1 \left[\frac{\partial}{\partial \alpha}(huu) + h\frac{\partial}{\partial \gamma}(\Omega u)\right] d\gamma$$

$$C_x = \frac{1}{\mathrm{Re}}\int_0^1 \left[\frac{\partial}{\partial \alpha}\left(h\frac{\partial u}{\partial \alpha}\right) + \left(\frac{1}{\epsilon^2}\right)\frac{1}{h}\left(\frac{\partial}{\partial \gamma}\left(A_v^* \frac{\partial u}{\partial \gamma}\right)\right)\right] d\gamma$$

$$X_p = E_u \int_0^1 h\left[\frac{\partial h}{\partial \alpha}\int_0^\gamma \rho\, d\gamma + h\left(\frac{\partial}{\partial \alpha}\int_0^\gamma \rho\, d\gamma\right) - \gamma\left(\frac{\partial h}{\partial \alpha}\right)\rho\right] d\gamma$$

The last term in the pressure equation, $\partial\Omega/\partial t$, at the surface should theoretically be zero. Since this is not true numerically, this term is evaluated and serves as a correction term for the predicted pressures (Hirt and Harlow[30]). This ordinary differential equation is solved iteratively by a successive overrelaxation technique. The pressures from the previous time step are used as the initial guess. The iteration directions are alternated to reduce mismatch between the pressure gradients near the two vertical boundaries. For each iteration the pressure gradient at either the downstream or the upstream wall is specified. These values are obtained from the previous time step. The iteration process is assumed to converge when the predicted values change less than 1%. This was found to occur within 15 iterations in most cases.

Model verification

The model was verified at first for an isothermal rectangular basin subject to a suddenly imposed surface shear stress. A constant value of eddy viscosity was used. The velocities predicted by the model away from the vertical walls were in excellent agreement with the analytical solution of the simplified momentum equation, i.e., when the nonlinear inertia and horizontal viscous terms are ignored (Sengupta and Lick[26]).

To verify the temperature predictions, we ran the model with parameters for Lake Cayuga, New York. The velocities were kept as zero, and surface heat exchange was specified from meteorological data. The results were compared with data and one-dimensional predictions of Lake Cayuga obtained from Sundaram and Rehm.[3] These are described in detail by Sinha.[31]

Transient response

Transient response of natural water bodies due to surface-imposed driving forces is important, since the steady state is usually never attained, because meteorological conditions vary with time. Moreover, the governing momentum and energy transport equations in this problem are coupled. Hence, verification of the momentum and energy transport solutions independently, as described in the previous section, does not necessarily guarantee agreement of the predicted results of the complete model with experimental data. This is primarily due to the complicated nature of the coupling, which depends on the interaction of turbulence and buoyancy. This section describes an attempt to experiment with these parameters with the aim of developing a better understanding of the flow.

Two simple cases were chosen for this purpose. The domain was a rectangular cutout, 1 km long and 30 m deep. These dimensions are approximately those of many small lakes, such as Lake Keowee (Sengupta *et al.*[5]). The vertical walls were assumed to be insulated. The initial conditions were zero velocities and a constant temperature of 10°C throughout the domain. A step input of 0.02 Pa shear stress and a temperature of 25°C were then suddenly applied to the surface while the bottom was held at a constant temperature of 10°C. Although a surface temperature gradient condition is more appropriate, the conditions are a simplified way to model the spring heating of temperate lakes. Additionally, specifying the temperatures rather than the gradients simplifies the boundary conditions and gives a clearer understanding of the internal dynamics of the basin. The turbulent Prandtl number was assumed to be unity for all cases, including the verification runs.

The only difference between the two cases was the formulation used in calculating eddy viscosities and diffusivities. In both cases the vertical eddy viscosity (or eddy diffusivity) is defined as

$$A_v = A_0(1 + \sigma \cdot \mathrm{Ri})^{-1}$$

where

A_0 = neutral value of $A_v = 0.01 A_{ref}$

σ = constant = 0.1

The Richardson number Ri is defined as

$$\mathrm{Ri} = \begin{cases} -\alpha_V g z^2 / w^{*2} & \text{for Case 1} \\ \dfrac{\alpha_V g(\partial T/\partial z)}{(\partial u/\partial z)^2} & \text{for Case 2} \end{cases}$$

where

α_V = the volumetric coefficient of expansion of water (obtained by linearization from the equation of state)

g = acceleration due to gravity

w^* = the friction velocity = $\sqrt{\tau/\rho}$

τ = the surface shear stress

Expressions for calculating α_V and Ri (Case 1) as well as the value of σ were obtained from one-dimensional simulations of Sundaram and Rehm[3] and Sengupta *et al.*[5] In Case 2 local gradients of the horizontal velocities were used to compute Ri, since these can be readily computed in a two-dimensional model.

Results and discussions

From the formulation of the problem it is expected that the velocities and temperatures would pass through a transient period and ultimately reach steady state. *Figures 3* and *4* show the development of the velocities and temperatures, respectively, with time for Case 1. The steady-state profiles of the same are shown in *Figures 5* and *6*. The numbers in parentheses represent grid points.

Figures 7–10 show the same for Case 2. Both cases were run with a time step of 100 s, being limited by the convective stability criterion. The values of velocities, temperatures, and eddy viscosities were printed out every 300 time steps till steady state was reached.

In Case 1 the velocities increase smoothly and reach steady state in 60 000 s (16.5 h). The temperatures (upstream) reach a maximum after 30 000 s (8.3 h), after which they reduce slightly and reach steady state. In Case 2, however, both horizontal velocities and temperatures at the upstream end exhibit rapid changes. (The words "upstream" and "downstream" are with reference to the direction of the surface shear stress and do not necessarily coincide with local flow directions.) The velocities reach an apparent steady state initially, but

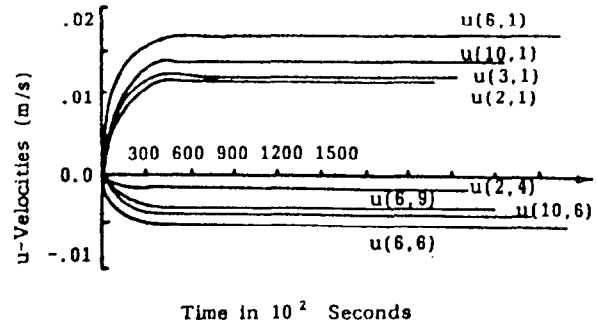

Figure 3 Variation of u (horizontal) velocities with time for Case 1

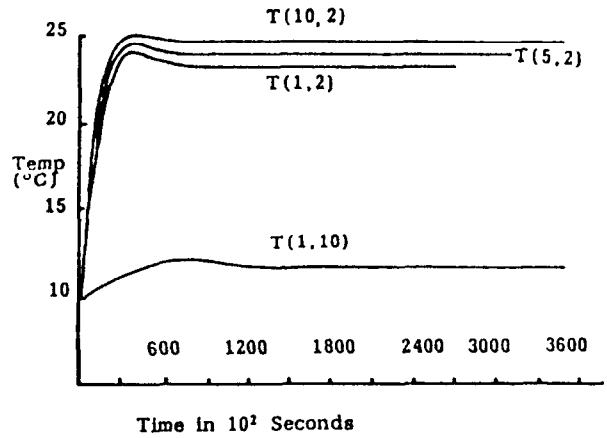

Figure 4 Variation of temperatures with time for Case 1

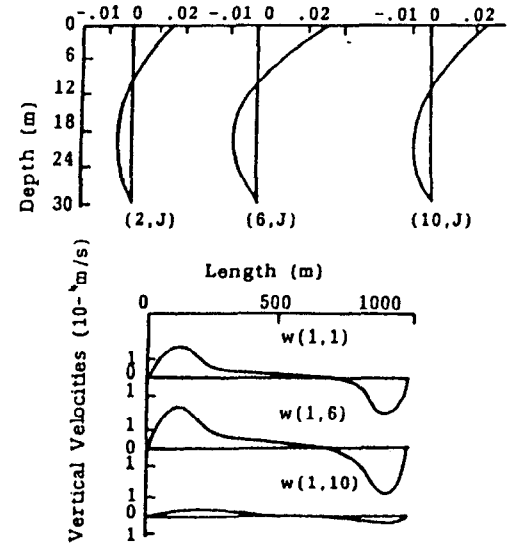

Figure 5 Horizontal and vertical velocities at steady state for Case 1

after 120 000 000 s they increase rapidly to reach the true steady state. The fluctuation in temperatures, although similar to Case 1, is more pronounced. Furthermore, the increase in velocities occurs concurrently with the temperatures reaching near-steady-state values. Additionally, these changes are extremely pronounced near the upstream end and reduce in the downstream direction.

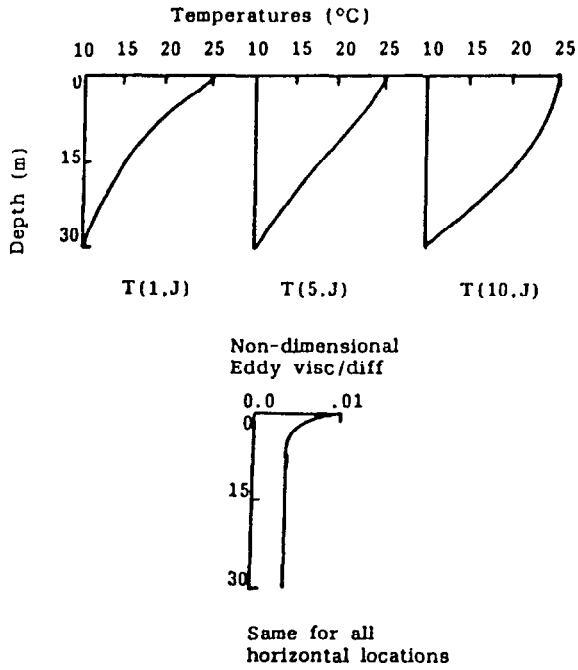

Figure 6 Temperature and nondimensional viscosities/diffusivities at steady state for Case 1

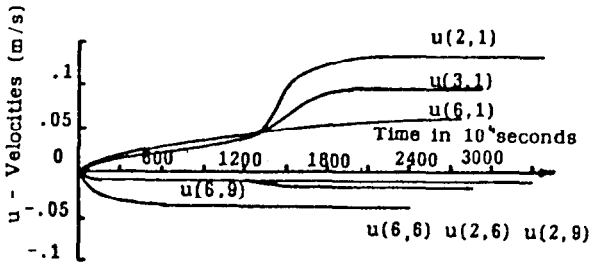

Figure 7 Variation of horizontal (u) velocities with time for Case 2

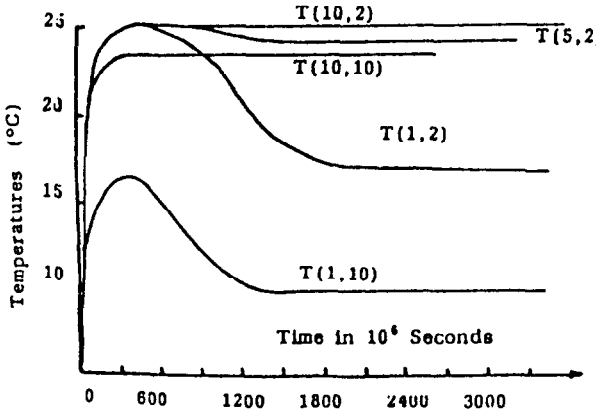

Figure 8 Variation of temperatures with time for Case 2

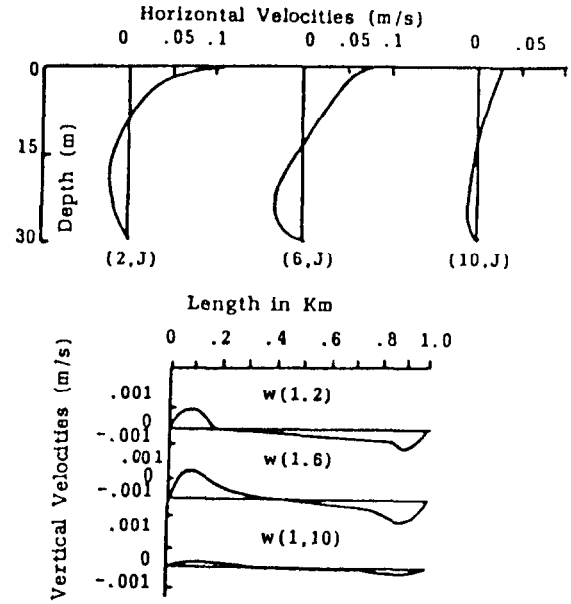

Figure 9 Horizontal and vertical velocities at steady state for Case 2

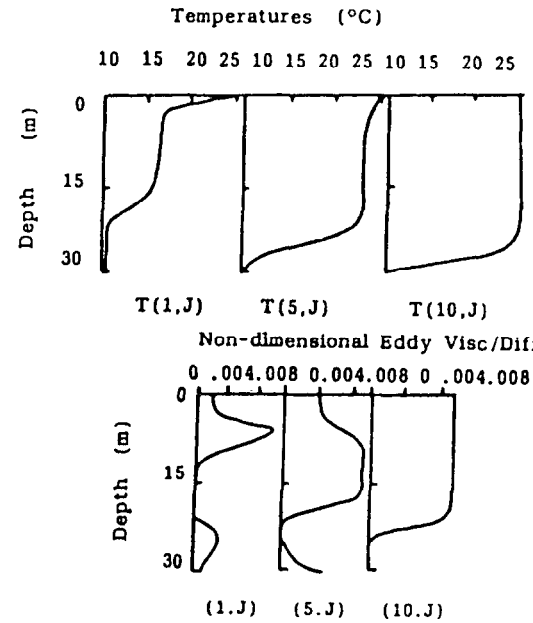

Figure 10 Temperatures and eddy viscosities/diffusivities at steady state for Case 2

A comparison of the steady-state velocity and temperature profiles for the two cases (*Figures 5, 6, 9,* and *10*) shows significant differences between the upstream and downstream end profiles for Case 2. These differences are smaller for Case 1.

A comparison of *Figures 7* and *8* suggests a correlation between the velocities and temperatures with respect to convective and diffusive time scales. A convective time scale may be defined as the time required for a mass of fluid to go around the domain and return to its original position. For a mass of fluid originating near the corner of the surface and the vertical upstream wall, the convective time scale was estimated as 110 000 s for Case 2. The diffusive time scale is determined solely by the local values of eddy viscosity (or

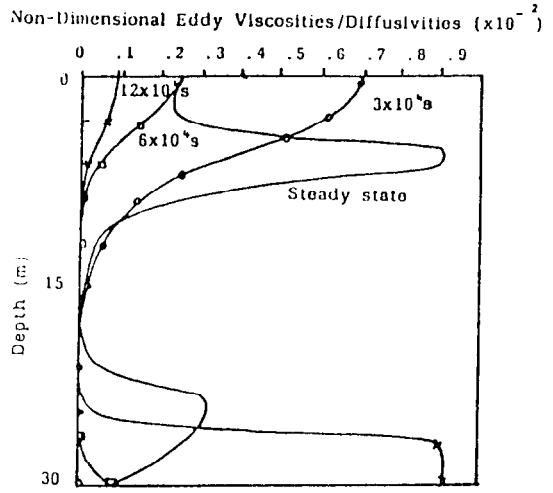

Figure 11 Eddy viscosity/diffusivity profiles at $(1, j)$ for Case 2

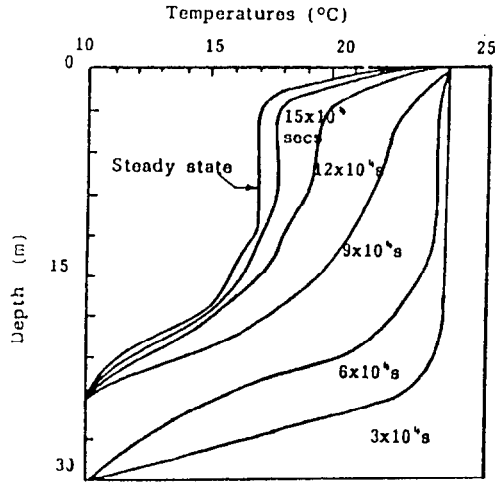

Figure 12 Temperature profiles at $(1, j)$ for Case 2

diffusivity). *Figures 11* and *12* show the eddy viscosity and temperature profiles with time for Case 2. The downstream profiles attained steady state almost instantaneously.

We will try to explain the sudden changes by focussing our attention on the effect of eddy viscosities and diffusivities due to interaction between temperature and velocity gradients. There are two predominant processes taking place in the domain. The first one is the diffusion of heat and momentum from the surface to the bottom, the magnitude of which is related directly to the values of the eddy diffusivities and viscosities. The second phenomenon is the transport of heat and momentum due to convection.

During the initial stages the diffusive process dominates. However, fairly soon the presence of vertical end walls causes the local flow direction to be reversed in the lower layers, giving rise to recirculation and associated convective effects. At the upstream end of the domain, recirculation causes cold fluid from the bottom layers (the bottom layers cool due to heat exiting through the bottom surface) to mix with the warmer fluid near the surface. This process is initiated after a time period equal to the previously defined convective time scale and explains the sudden drop in temperatures seen in *Figure 8*. Moreover, the eddy viscosities and diffusivities are directly related to the local velocity gradients in Case 2. Since the surface is held at a constant temperature, the presence of a mass of cold fluid just below the surface increases the vertical gradient of the temperature in this region, as seen in *Figure 12*. This results in an increase in the local Richardson number, leading to a drop in the surface eddy viscosities and diffusivities near the upstream end, as seen in *Figure 11*. Lowering the eddy coefficients reduces the local surface heat flux and increases the vertical gradient of the horizontal velocities. Since the surface shear stress is constant and the velocities below the surface are determined by the inertia of the recirculating fluid, the surface velocities have to increase.

This explanation is fortified by the fact that the maximum rate of change of the temperatures coincides closely with the maximum rate of change of the horizontal velocities. We can see this by comparing *Figures 7* and *8*. However, the comparisons should be used with caution, since the temperatures are computed at half grid points, which are 50 m away from the nearest full grid point used for computing u-velocities.

In Case 1 the eddy coefficients are unaffected by local velocity and temperature gradients. Hence, variations of these coefficients in the horizontal direction cannot be reproduced. This reduces the difference between the upstream and downstream velocity profiles in this case. The maxima in the upstream temperatures occur due to reasons mentioned before. However, local temperature gradients are not used in estimating eddy viscosities. Thus, the eddy viscosity near the surface does not change. Therefore no sudden increase is noted in the velocities.

Conclusions

It has been demonstrated that local mixing processes play a significant role in the transient and steady-state responses of stratified reservoirs. The use of local velocity and temperature gradients in calculating eddy coefficients alters the predicted results considerably. This is portrayed in the differences between the two cases. The turbulence model used in Case 2 is superior, since both horizontal and vertical variations of turbulence can be represented. The validity of this turbulence model and the occurrence of sudden changes in temperatures and velocities together with the predicted multiple thermoclines are, however, subject to experimental verification. The stratified lid-driven cavity-flow experiments of Koseff and Street[7] do not indicate any sudden changes in velocities or temperatures. However, their experiments were conducted in a square enclosure with an initially linearly stratified fluid. Hence, a direct comparison cannot be made with the present numerical solutions.

The values of aspect ratio, shear stress, and temperature differences used for this study may change, depending on the topography, geographical location, and meteorological conditions of the water body in question. Moreover, it is difficult to obtain extensive reliable data from natural reservoirs. Hence, the authors feel that controlled laboratory experiments are necessary to verify the turbulence closures.

Nomenclature

A_h	horizontal eddy viscosity
B_h	horizontal eddy diffusivity
A_v	vertical eddy viscosity
B_v	vertical eddy diffusivity
A_{ref}, B_{ref}	reference eddy viscosity and eddy diffusivity
g	acceleration due to gravity
h	local depth
L	length of domain
H	maximum depth of domain
p	local fluid pressure
P_s	surface pressure due to rigid-lid assumption
t	time
T	temperature
u, w	horizontal and vertical velocities
Ω	transformed vertical velocity
x, α	actual and transformed horizontal coordinates
z, γ	actual and transformed vertical coordinates
ρ	density
τ	surface shear stress
ref	subscript used to denote reference quantities
*	superscript used to denote nondimensional quantities
~	superscript used to denote dimensional quantities

References

1 Huppert, H. E. and Linden, P. L. 'On heating a stable salinity gradient from below', *J. Fluid. Mech.*, 1979, **95**, 431–464

2 Brocard, D. N. and Harleman, D. R. F. 'Two layer model for shallow horizontal convective circulation', *J. Fluid. Mech.*, 1980, **100**, 129–146

3 Sundaram, T. R. and Rehm, R. G. 'Formation and maintenance of thermocline in temperate lakes', *AIAA J.*, 1970, **9**(7), 1322–1329

4 Henderson-Sellers, B. 'New formulation of eddy diffusion thermocline models', *Appl. Math. Modelling*, 1985, **9**, 441–447

5 Sengupta, S., Nwadike, E., and Lee, S. 'Long term simulation of stratification in cooling lakes', *Appl. Math. Modelling*, 1981, **5**, 313–320

6 Sinha, S. K. and Sengupta, S. 'An investigation of destratification in enclosed basins due to surface shear', *ASME Wint. Ann. Meeting*, 1986

7 Koseff, J. R. and Street, R. L. 'Circulation structure in a stratified cavity flow', *ASCE J. Hyd. Eng.*, 1985, **111**(2)

8 Rhee, H., Koseff, J. R., and Street, R. L. 'Flow visualization of a recirculating flow by rheoscopic liquid and liquid crystal techniques', *Expt. in Fluids*, 1984, **2**, 57–64

9 Kranenburg, C. 'Wind induced entrainment in a stably stratified fluid', *J. Fluid Mech.*, 1984, **145**, 253–273

10 Kranenburg, C. 'Mixed layer deepening in lakes after wind setup', *ASCE J. Hyd. Eng.*, 1985, **111**(9), 1279–1297

11 Kit, E., Berent, E., and Vajda, M. 'Vertical mixing induced by wind and a rotating screen in a stratified fluid in a channel', *J. Hyd. Res.*, 1980, **18**(1), 35–58

12 Wu, J. 'Wind induced entrainment across a stable density interface', *J. Fluid. Mech.*, 1973, **61**(2), 275–287

13 Wu, J. 'A note on the slope of the density interface between two stably stratified fluids under wind', *J. Fluid Mech.*, 1977, **81**, 335–339

14 Monismith, S. G. 'Dynamic response of stratified reservoirs to surface shear stress', *Report No. UCB/HEL-83/05, Hyd. Eng. Lab., Univ. of California, Berkeley*, 1983

15 Chasechkin, J. D. 'Experimental studies on the mixed layer in stratified liquids', *IAHR Symp. on Stratified Flow, Trondheim, Norway*, 1980, pp. 783–790

16 Sinha, S. K. 'An experimental investigation of recirculation and destratification in lid-driven cavity flows', *Diss., Univ. of Miami, Dept. of Mech. Eng.*, 1986

17 Mortimer, C. H. 'Water movements in lakes during summer stratification. Evidence from the distribution of temperature in Windmere', *Phil. Trans. Roy. Soc., London*, 1952, **B236**, 355–404

18 Wedderburn, E. M. 'The temperature seiche: observations in the Madusee', *Trans. Roy. Soc., Edinburgh*, 1911, **47**, 619–642

19 Wedderburn, E. M. 'Temperature observations in Loch Earn with a further contribution to the hydrodynamical theory of temperature seiches', *Trans. Roy. Soc., Edinburgh*, 1912, **48**

20 Torrance, K., Davis, R., Eike, K., Gill, P., Gutman, D., Hsui, A., Lyons, and Zien, H. 'Cavity flows driven by buoyancy and shear', *J. Fluid. Mech.*, 1972, **51**, 221

21 Young, D. L., Liggett, J. A., and Gallagher, R. H. 'Steady stratified circulation in a cavity', *ASCE J. Eng. Mech. Div.*, 1976, **102**(EM6), 1009–1023

22 Simons, T. J. 'Circulation models of lakes and inland seas', *Can. Bull. Fish. Aquat.*, 1980, **SCI 203**, 146

23 Davies, A. M. 'Numerical modelling of stratified flow: a spectral approach', *Continental Shelf Res.*, 1983, **2**, 275–300

24 Cheng, R. T., Powell, T. M., and Dillon, T. M. 'Numerical models of wind-driven circulation in lakes', *Appl. Math. Modelling*, 1976, **1**, 141–158

25 Davies, A. M. 'On computing flow in a stratified sea using the Galerkin method', *Appl. Math. Modelling*, 1982, **6**, 347–362

26 Sengupta, S. and Lick, W. A. 'Numerical model for wind driven circulation and temperature fields in lakes and ponds', *Case Western Reserve Univ., Report FTAS/TR-74-99*, 1974

27 Sengupta, S. 'A three dimensional rigid-lid model for closed basins', *ASME J. Heat Transfer*, 1977, **99**, 656–662

28 James, I. D. 'A three dimensional numerical shelf-sea front model with variable eddy viscosity and diffusivity', *Continental Shelf Res.*, 1984, **3**, 69–98

29 Hirt, C. W. and Harlow, F. H. 'A general corrective procedure for the numerical solution to initial-value problems', *J. Comp. Phys.*, 1967, **2**

30 Sinha, S. K. 'A two dimensional numerical investigation of buoyancy and shear driven flows in natural bodies of water', *M.S. Thesis, Univ. of Miami, Dept. of Mech. Eng.*, 1981